Synthesis and Characterization of Nylon 6/Clay Nanocomposites Prepared by Ultrasonication and In Situ Polymerization

C. P. McAdam, N. E. Hudson, J. J. Liggat, R. A. Pethrick

Department of Pure and Applied Chemistry, University of Strathclyde, Glasgow G1 1XL, United Kingdom

Received 13 July 2006; accepted 6 September 2006
DOI 10.1002/app.25599
Published online 7 February 2008 in Wiley InterScience (www.interscience.wiley.com).

ABSTRACT: Nylon 6 nanocomposites were prepared by the *in situ* polymerization of ε-caprolactam with ultrasonically dispersed organically modified montmorillonite clay (Cloisite 30B®). Dispersions of the clay platelets with concentrations in the range 1–5 wt % in the monomer were characterized using rheological measurements. All mixtures exhibited shear-thinning, signifying that the clay particles were dispersed as platelets and forming a ''house of cards'' structure. Samples with Cloisite concentrations above 2 wt % showed a drop in viscosity between the initial shearing and repeated shearing, indicative of shearing breaking down the initial ''house of cards'' structures formed on sonication. DMTA measurements of the samples showed an increase in the β-relaxation temperature with increasing clay concentration. The bending modulus, at temperatures below T_g, showed an increase with increasing clay concentration up to 4 wt %. X-ray diffraction measurements showed that all nylon 6/Cloisite 30B samples were exfoliated apart from the 5 wt %, which showed that some intercalated material was present. The nylon crystallized into the α-crystalline phase, which is the most thermodynamically stable form. Preference for this form may be a consequence of the long time associated with the postcondensation step in the synthesis or the influence of the platelets on the nucleation step of the crystal growth. DSC measurements showed a retardation of the crystallization rate of nanocomposite samples when compared with that of pure nylon 6, due to the exfoliated clay platelets hindering chain movement. This behavior is different from that observed for the melt-mixed nylon 6/clay nanocomposites, which show an enhancement in the crystallization rate. J Appl Polym Sci 108: 2242–2251, 2008

Key words: nylon; crystallization; glass transition; nanocomposites; clay

INTRODUCTION

Nanocomposites based on the dispersion of clay particles in a polymer were first created by Fujiwara and Sakamoto[1] using nylon 6, and later optimized by researchers at the Toyota Motor Company[2,3] in Japan. It was observed that these materials had double the tensile modulus, a 50% increase in tensile strength, and an increase of 80°C in the heat distortion temperature range when compared with the pure polymer. Other advantages of the nanocomposites were a reduction in gas permeability, flammability, and water absorption.

Since these initial studies, there have been a considerable number of papers published on nanocomposites (for example, see Refs. [4–12]). Many of the publications have used montmorillonite as the preferred clay as it has one of the highest aspect ratios of naturally occurring clay particles. Montmorillonite is an aluminosilicate and its structure consists of a sheet of octahedral aluminum oxide, AlO_6, sandwiched between two layers of tetrahedral silicon oxide, SiO_4, to form a platelet structure. Each platelet can have a length or breadth of up to 1 μm but are only 1 nm thick. Montmorillonite is a naturally occurring form of clay in which certain of the aluminum ions have been exchanged with other cations, typically Fe, Mg, or Li to create a net negative charge at the platelet surface. In nature, these sites are the location for cations such as sodium, which balance the negative charge. The platelets form small, organized stacks called tactoids, in which the exchangeable cations fit in between the platelets and hold them together. The commercial Cloisite materials are a form of the clay in which the cations have been exchanged with organic cations, resulting in an increase in the interplatelet separation allowing access of the surrounding monomer or polymer into the galleries formed by the clay platelets.

Despite the organic surface modification, it is found to be still relatively difficult to achieve the exfoliated dispersed structure that will give maximum enhancement of properties. Three types of structure are possible within polymer/clay composite systems: phase separated microcomposites, where no separation of clay platelets has occurred; intercalated structures in which some polymer has penetrated the interlayer galleries of the clay tactoids increasing the

Correspondence to: J. J. Liggat (j.j.liggat@strath.ac.uk).
Contract grant sponsor: EPSRC.

silicate layer separation; and exfoliated structures containing completely separated and orientated clay platelets. Commonly, a mixed structure of exfoliated and intercalated nanostructures is present in many nanocomposite materials.

Nylon 6/clay nanocomposites have been produced by either melt mixing[13–19] or *in situ* polymerization.[20–24] Melt mixing involves shearing nanoclay, using a twin-screw extruder, directly into molten nylon 6 to disperse the platelets throughout the matrix. *In situ* polymerization was the original method used[1,2] by Toyota Research Laboratories, montmorillonite being intercalated using 12-aminolauric acid. This process was subsequently improved by Kojima et al.[20,21]

Studies at Strathclyde and elsewhere have identified that ultrasound can aid exfoliation[25–27] and allows significant enhancement of the physical properties to be achieved. Ultrasonication has also been used to synthesize polymer/clay nanocomposites with polymers such as poly(propylene-*co*-styrene),[28] poly(methyl methacrylate),[27,28] polyimide,[29] and poly (dicyclopentadiene).[30]

The crystalline structure of nylon 6 is known to predominantly favor the α-form, in which antiparallel polyamide chains are situated such that the amide linkages and methylene groups lie in the same plane, allowing maximization of hydrogen bonding. The addition of clay platelets to nylon 6 is known to promote the formation of the less thermodynamically stable γ-crystalline form, in which parallel chains require the amide linkages to twist approximately 60° out of the plane of molecular sheets of nylon 6 chains. The majority of studies into the crystalline morphology of nylon 6/clay nanocomposites have used melt mixed samples.[31–33] Several papers[34–36] have compared the crystalline forms of nanocomposites prepared via *in situ* polymerization and melt mixing. It was noted that regardless of the method of synthesis, the γ-form would always be preferentially formed over the α-form. At the polymer–clay interface, γ-crystallites are formed whereas α-crystallites are present in the bulk of the nanocomposite.

In this paper, we explore the nature of the dispersion that is created when ultrasound is used to aid dispersion of the clay platelets and the physical properties of the materials produced after *in situ* polymerization.

EXPERIMENTAL

Materials

Nylon 6 was synthesized using ε-caprolactam (99%), supplied by Aldrich. It was used in the form of white, crystalline pellets and has a melting point of 68°C. 6-Aminocaproic acid (98%) was supplied by Aldrich. It is a white, crystalline powder and has a melting range of 207–210°C. Cloisite 30B® was received from Southern Clay Products, Texas. It is an aluminosilicate clay that contains methyl tallow bis-2-hydroxyethyl quaternary ammonium chloride as an organic modifier. The tallow is a long hydrocarbon chain group consisting of 65% C_{18}, 30% C_{16}, and 5% C_{14}. The surface modification concentration is 90 mEq/100 g and the clay has a water content of approximately 2% (w/w).

Dispersion of clay in monomer

Nylon 6/Cloisite 30B nanocomposite samples were made in two main stages. The first stage was dispersion of Cloisite 30B in molten ε-caprolactam using sonication and the second was polymerization of the resulting monomer/clay mixture to form the nanocomposite.

Solid ε-caprolactam was heated at 85°C until molten. The liquid ε-caprolactam was placed in a preheated container and the required amount of clay was added. The mixture was stirred using a Eurostar IKA-WERKE stirrer at 250 rpm and sonicated using a Cole-Palmer ultrasonic processor with a 1/8-in. titanium sonic probe immersed in the liquid, for 15 min at 30% power. Heat generated by sonication process was sufficient to maintain ε-caprolactam in liquid phase.

In situ polymerization

Approximately 12 g of the ε-caprolactam/Cloisite 30B sonicated mixture was placed in a reaction vessel. To this mixture, 1.2 g of 6-aminocaproic acid (10% (w/w)) was added as an initiator for the polymerization reaction. In the case of nanocomposite samples, the 6-aminocaproic acid was added to the vessel before the ε-caprolactam/Cloisite 30B mixture. The vessel was held in a heating block, which was preheated to 220°C. The contents of the tube were flushed with nitrogen and the reaction mixture was heated at 220°C until the initiator had completely dissolved into the monomer/clay mixture. The temperature of the reaction mixture was then raised to 250°C for 5 h. After 5 h at 250°C, the product was allowed to solidify in the reaction vessel overnight. The product was then heated to 200°C under a nitrogen blanket for 8 h. This was a postcondensation reaction step designed to further increase the nylon 6 molecular weight in the resulting polymer/clay nanocomposite.

Rheology

Measurements were carried out on a CSL^2 Carri-Med rheometer (TA Instruments, Leatherhead) using a cone and plate geometry with a truncated 4 cm, 2° steel cone. Measurements were made using a shear rate range of 2–200 s^{-1} at a temperature of 75°C.

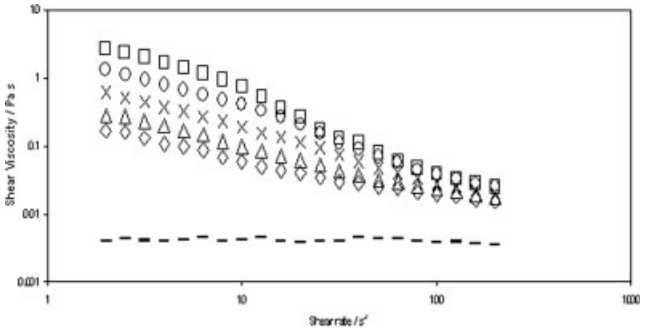

Figure 1 Shear viscosity versus shear rate measured at 75°C for sonicated dispersions of Cloisite 30B in ε-caprolactam, illustrating the increase in viscosity as the clay concentration is increased. This data represents the initial runs performed on each sample. (−) 0 wt %; (◇) 1 wt %; (△) 2 wt %; (×) 3 wt %; (○) 4 wt %; (□) 5 wt %.

X-ray diffraction

X-ray samples were examined using a Siemens D500 Diffraktometer with copper wavelength. The nylon 6/clay nanocomposite disc was placed in the sample holder and data recorded through angles from 1.5° to 30° with a step-size of 0.05 every 4 s.

Dynamic mechanical thermal analysis

DMTA measurements were made using a Polymer Laboratories Dynamic Mechanical Thermal Analyzer MKIII, at a frequency of 1 Hz, a strain of ×4; scanning rate of 4°C min^{-1} and the samples were clamped with a torque of 40*N*. Each polymer/clay nanocomposite sample was dried for 24 h in a vacuum at 80°C prior to measurement.

Differential scanning calorimetry

A TA Q-1000 Differential Scanning Calorimeter was used for all DSC work on nylon 6 and nylon 6/cloisite 30B nanocomposite samples. For nonisothermal work, each sample was held at −25°C for 1 min, heated from −25°C to 250°C at 10°C min^{-1}, held for 1 min at 250°C, cooled from 250°C to −25°C at 10°C min^{-1}, held for 1 min at −10°C and subsequently heated from −10°C to 250°C at 10°C min^{-1}. For the isothermal experiment, samples were ramped from 25°C to 250°C at 20°C min^{-1}, held for 1 min to ensure melting, and then rapidly cooled at 40°C min^{-1} to 195°C, where they were allowed to crystallize for 60 min. The chosen crystallization temperature was determined through a series of experiments conducted at various crystallization temperatures.

Gel permeation chromatography

Measurement of the molecular weight of nylon 6/clay nanocomposite samples was performed by Rapra Technology Ltd. using a Polymer Laboratories GPC120, with PL GPC-AS MT autosampler and Plgel guard plus 2× mixed bed-B columns. 1,3-cresol with antioxidant was used as the solvent with a flow rate of 0.8 mL min^{-1} at 115°C.

RESULTS AND DISCUSSION

Rheology of ε-caprolactam/clay dispersions

A rheological analysis of the sonicated ε-caprolactam/clay dispersions allows an investigation into the degree of exfoliation present in each sample (Fig. 1). Each sample displayed enhancement of viscosity and shear thinning, compared with pure ε-caprolactam, indicating that the clay platelets are exfoliated in the liquid monomer. Shear thinning occurs as the platelets align themselves in the direction of the applied shear; hence, a lowering of the viscosity is observed with increasing shear rate. This effect has also been observed in rheological studies with polyurethane[25] and poly(methyl methacrylate)[27] nanocomposites.

Montmorillonite clay platelets are charged species with negative charges present on their surface (opposed by the cationic organic modifier species) and positive charges round their edge. In dispersion, exfoliated platelets can interact electrostatically, as they are sonicated, to build up a ''house of cards'' structure. Figure 2 displays the shear stress versus shear rate data of the Cloisite 30B in ε-caprolactam sonicated dispersions. The 3, 4, and 5 wt % dispersions each show a significant peak in the low shear rate range between 0 and 50 s^{-1}. This peak is attributed to a structural change in the sample, most likely the elastic deformation and the subsequent breakdown of the ''house of cards'' as a critical shear stress is attained. The idea of an elastic deformation and a subsequent breakdown of the platelet network structure has been proposed by Li et al.[37] It is

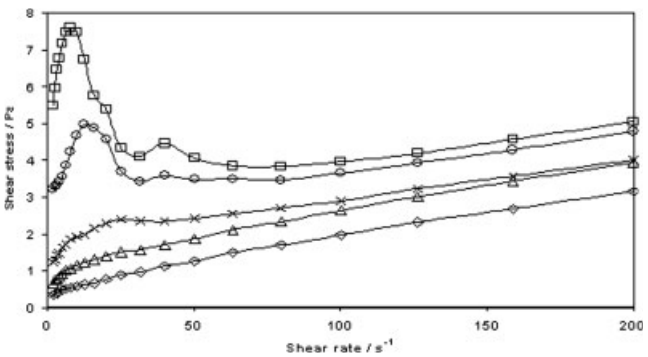

Figure 2 Shear stress versus shear rate measured at 75°C for sonicated dispersions of Cloisite 30B in ε-caprolactam. The dispersions each display a yield stress, and the 3, 4, and 5 wt % samples each show a significant peak, which represents the elastic deformation of the ''house of cards'' prior to its breakdown. (◇) 1 wt %; (△) 2 wt %; (×) 3 wt %; (○) 4 wt %; (□) 5 wt %.

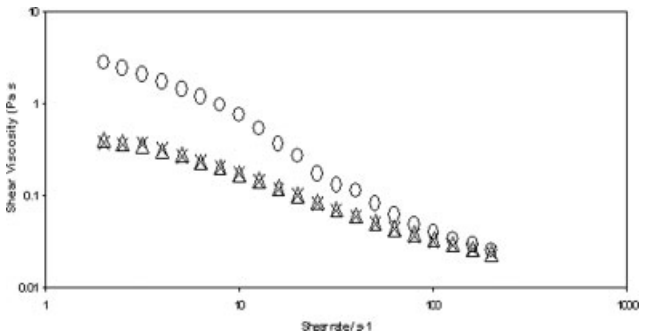

Figure 3 Shear viscosity versus shear rate for a 5 wt % Cloisite 30B in ε-caprolactam dispersion at 75°C to demonstrate the drop in viscosity observed in the sample between initial shearing and immediate repeat shearings. (○) Initial Run; (△) and (×) are immediate repeat measurements of the same sample.

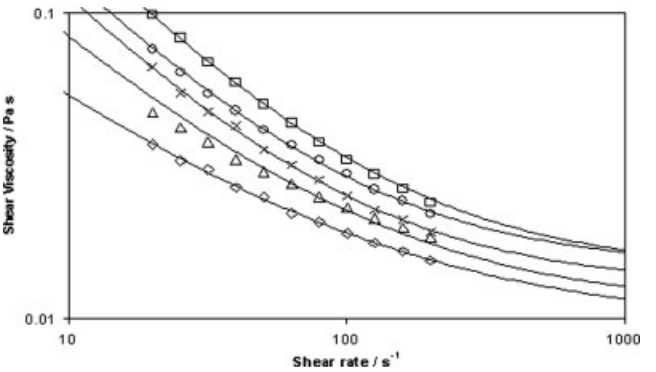

Figure 4 Shear viscosity versus shear rate for immediate repeat run data. The high shear rate data fitted to the Sisko model. The parameters determined are shown in Table I. (◇) 1 wt %; (△) 2 wt %; (×) 3 wt %; (○) 4 wt %; (□) 5 wt %.

theorized that when a nanocomposite is under strain there may be an elastic deformation region where the structure is not broken down. However, when the strain is increased the network structure is broken down and the network is irrecoverable.

The initial, second, and third run data of the 5 wt % are shown in Figure 3. It was observed, on samples with concentrations from 2 to 5 wt %, that the initial run gave a higher viscosity that the immediate repeat. The difference in viscosity, between the initial and two immediate repeat runs, is further evidence that the ''house of cards'' structure has been destroyed.

The immediate repeat run data at high shear rates can be fitted to the Sisko model, $\eta = \eta_\infty + K_2(\dot{\gamma})^{n-1}$, where η_∞ is the viscosity at very high shear rate (when all structure is broken down), n is a power law index, and K_2 is a constant. The Sisko model provides a method of describing the relative rate of the reorientation of the clay platelets in the flow field. The values obtained from the parameters of the Sisko model are shown in Table I.

The second repeat run data at high shear rates, as shown in Figure 4, can be fitted to the Sisko model,[38] $\eta = \eta_\infty + K_2(\dot{\gamma})^{n-1}$, where η_∞ is the viscosity at very high shear rate (when all structure is broken down), n is a power law index, and K_2 is a constant. The Sisko model provides a method of describing the relative rate of the reorientation of the clay platelets in the flow field. The values obtained from the parameters of the Sisko model are shown in Table I. As these have been obtained by extrapolating a limited set of experimental data (which in itself in subject to some error, estimated to be no more than 5%), they should be regarded as good estimates. In particular, the curve for 5 wt % probably approaches that for 4 wt % too closely.

The values obtained for the power law index, n, indicate the highly shear thinning behavior of these suspensions, particularly at the higher concentrations. The constant, K_2, is sometimes referred to as the consistency coefficient, and as shown in Figure 5, is approximately linear with concentration. The values obtained for the high shear rate viscosity enable one to gain some insight into particle shape, by extending the work of Einstein[39,40] on the viscosity of dilute suspension of spheres, and generalizing his equation to $\eta = \eta_\infty (1 + K_3 c)$, where c is the concentration and K_3 is a shape factor. As seen in Figure 5,

TABLE I
The Parameters Determined from Fitting the Immediate Repeat Data to a Sisko Model at High Shear Rates

	Concentration				
Parameter	1%	2%	3%	4%	5%
η_∞/Pa s	0.0096	0.0109	0.0129	0.0148	0.0145
K_2/Pa s^n	0.204	0.452	0.803	0.945	1.300
n	0.334	0.206	0.093	0.090	0.084

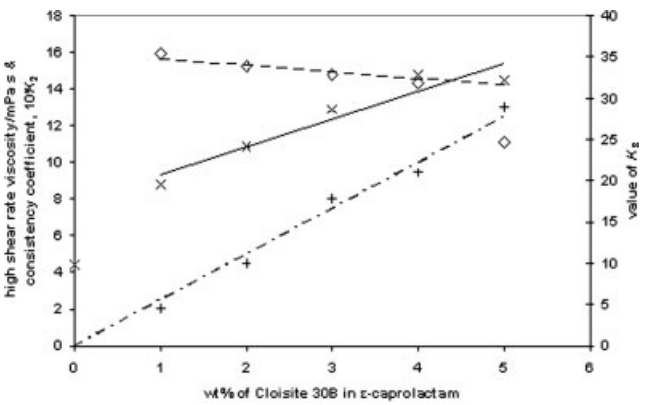

Figure 5 High shear rate viscosity, η_∞ (×); consistency coefficient, $K_2 \times 10$ (+); and shape factor, K_3 (◇), as functions of the concentration in wt % of Cloisite 30B in ε-caprolactam.

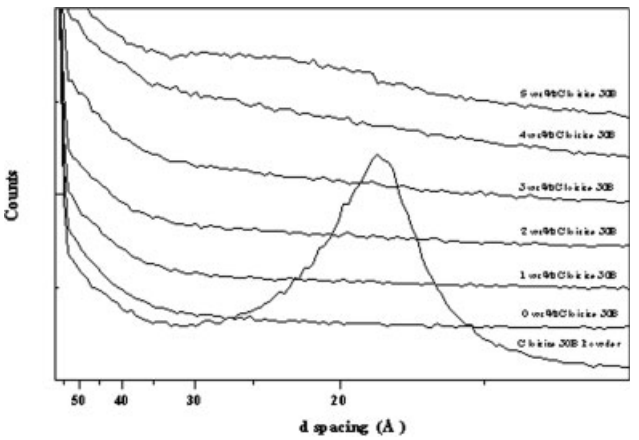

Figure 6 X-ray diffraction traces of nylon 6/Cloisite 30B nanocomposite samples with clay concentrations from 0 to 5 wt % and polymerized at 250°C with a postcondensation step at 200°C. The trace for pure Cloisite 30B powder is also shown for reference.

at least for most values of concentration, K_3 has an approximate value of 33, when compared with $2.5c/\theta$ (where θ is the corresponding volume fraction) for a sphere. This indicates that the clay particles are keeping their long slender shape, and not forming structures that are more spherical.

X-ray diffraction

Although the sonicated ε-caprolactam/clay dispersions showed shear thinning behavior and enhanced viscosity, indicating that some exfoliation had taken place, X-ray diffraction measurements were performed to determine the platelet morphology of the polymerized nylon 6/clay nanocomposite samples, the results of which are shown in Figure 6. X-ray diffraction is a useful tool in the study of polymer/clay nanocomposites. It is used to measure the interlayer distance, or *d* spacing, between the clay platelets. This distance is represented by a peak in an XRD scan at a particular *d* spacing value. Figure 6 shows that exfoliation of the clay platelets at concentrations of 1–4 wt % Cloisite 30B in nylon 6 has been achieved using *in situ* polymerization of ε-caprolactam/clay mixtures. The Cloisite 30B scan shows a peak at approximately 18.4 E and there are no peaks observed in the scans for the 1–4 wt % samples, indicating that complete exfoliation of the clay platelets has occurred. However, the 5 wt % sample shows a very broad peak in the scan within the range 32.7–16.1 Å. This indicates that the clay platelets within this sample are not completely exfoliated and there is some intercalated material present. As the concentration of clay increases, it becomes more difficult to fully exfoliate the sample because of the presence of increasing amounts of clay platelets. So this is an expected result.

Figure 7 gives information about the crystalline regions within the polymer nanocomposite samples. The plot for the pure nylon 6 sample shows two main peaks at 4.48 and 3.76 Å (equivalent to 2θ angles of 19.8° and 23.7°), which represent the distances between the sheets of polymer chains and the distance between individual chains within each sheet respectively, in the α-crystalline form of the polymer. The sonicated dispersion of clay into the nylon 6 does not have any effect on the crystalline form of the polymer. Previous work[31–33] has reported that addition of clay into nylon 6 has caused the crystalline form of the polymer to change from α to γ because of a limitation in mobility of the polymer chains. However, studies[41] have also shown that the crystallization temperature has a large influence on which crystalline form of nylon 6 is preferentially formed. At temperatures above 190°C, the crystallization rate of the α-form, which is the most stable crystalline form of nylon 6, is faster. Hence, in the data shown in Figure 7, the samples have all formed the α-form because the synthesis process used to make these samples involved a postcondensation stage, where the samples were held at a constant temperature of 200°C for 8 h. During this time, the polymer chains within the samples can align themselves into the more thermodynamically stable α-form, even when the concentration of clay is relatively high, such as at 5 wt %. An alternative explanation could be that the crystal growth is nucleated by the surface of the clay. The nucleation would involve favorable interaction between the polymer chains and the surface leading to growth of the lower energy form of the crystal. Observation of the α-form is in contrast with previous observations[31–36] of the structure of nylon, where the γ-form appears to have been the preferred structure.

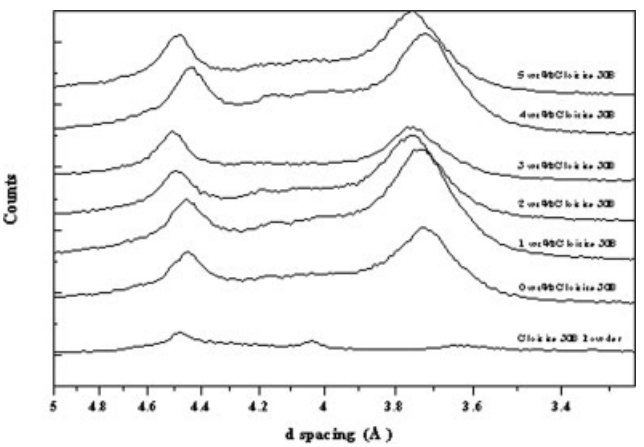

Figure 7 X-ray diffraction traces of the crystalline region within nylon 6/Cloisite 30B nanocomposite samples with clay concentrations from 0 to 5 wt % and polymerized at 250°C with a postcondensation step at 200°C.

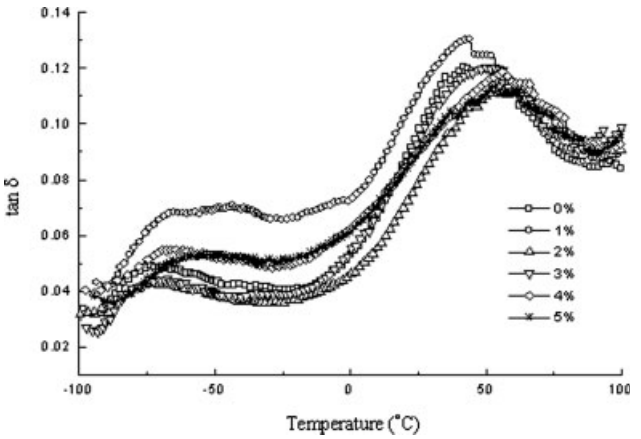

Figure 8 DMTA tan δ versus temperature curve for nylon 6/Cloisite 30B nanocomposite samples with clay concentrations from 0 to 5 wt %. (□) 0 wt %; (○) 1 wt %; (△) 2 wt %; (▽) 3 wt %; (◇) 4 wt %; (*) 5 wt %.

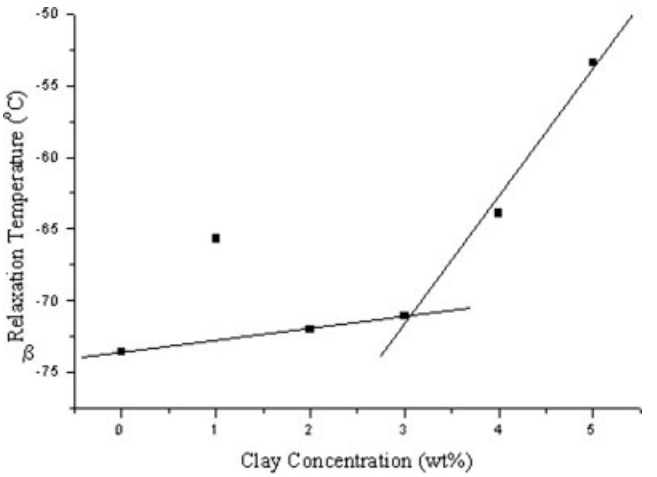

Figure 10 β-relaxation temperature versus clay concentration for nylon 6/Cloisite 30B nanocomposite samples obtained from DMTA measurements.

Dynamic mechanical thermal analysis

Figure 8 presents the tan δ versus temperature data obtained from DMTA measurements of the nanocomposite samples synthesized using ultrasonication and *in situ* polymerization. The data shows shifts in the positions of the glass transition and β-relaxation temperature upon the addition of nanoclay, compared with pure nylon 6.

Figure 9 shows a very pronounced increase in T_g with increasing clay concentration. The presence of the clay in the amorphous regions of the polymer structure will have the effect of restricting chain mobility and reducing free volume. The T_g is the temperature where the free volume is sufficient that the coordinated segmental motion within polymer chains can occur. For chain motion to occur with clay present, the T_g will increase to a higher temperature. The scatter of some of the data points can be attributed to slight differences in the thermal histories of the samples. The decrease in T_g at 5 wt % after the general increase, with clay concentration, in the glass transition temperature may be due to the intercalated nature of the platelet morphology when compared with the exfoliated nature of the other samples. In contrast to these results, work by Pramoda et al.[42] has shown that addition of nanoclay to nylon 6 can have the effect of lowering the glass transition temperature rather than increasing it.

Excluding the point for 1 wt %, the β-relaxation temperature increases with clay concentration, as displayed in Figure 10. The β-relaxation is associated with localized motion in polymer chains of either a relatively small number of monomer units or motion of side chains. In the case of nylon 6, it could be associated with the onset of the motion of the amide

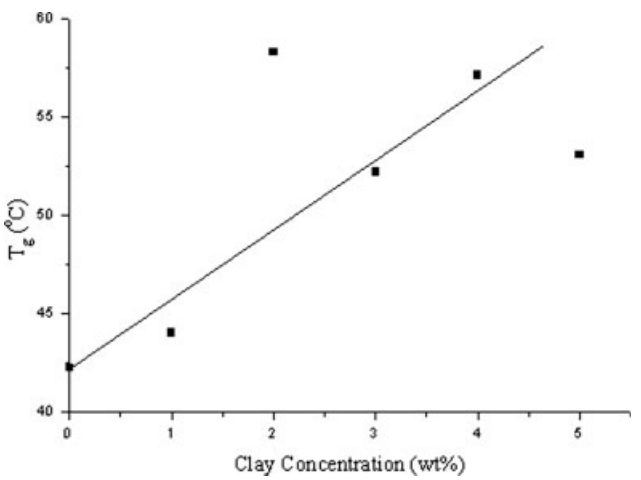

Figure 9 Glass transition temperature versus clay concentration for nylon 6/Cloisite 30B nanocomposite samples obtained from DMTA measurements.

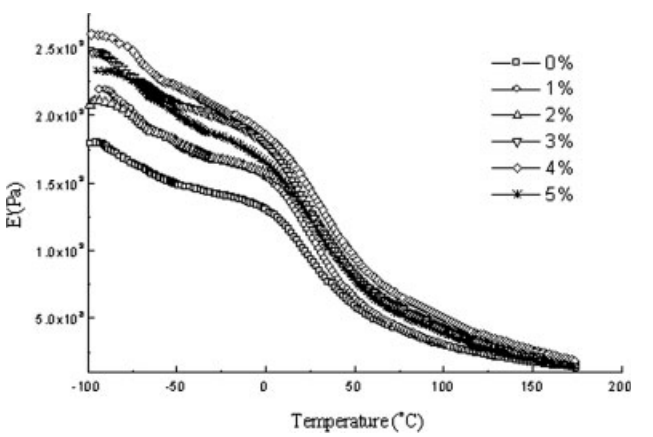

Figure 11 Bending modulus, E', versus temperature for nylon 6/Cloisite 30B nanocomposite samples with clay concentrations from 0 to 5 wt %. (□) 0 wt %; (○) 1 wt %; (△) 2 wt %; (▽) 3 wt %; (◇) 4 wt %; (*) 5 wt %.

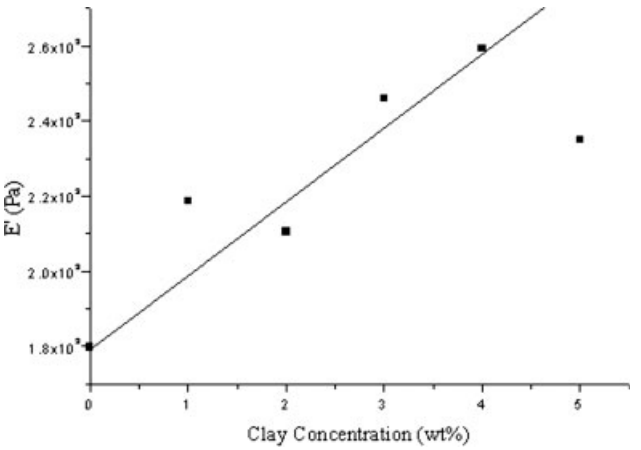

Figure 12 Bending modulus, E', versus clay concentration for nylon 6/Cloisite 30B samples with clay concentrations from 0 to 5 wt % measured at −95°C.

groups, carbonyl groups, or amine groups in each polymer chain. The work by Pramoda et al.[42] has detailed that the peak temperature of the β-relaxation shifted to a lower temperature as the moisture content of the nylon was increased. The water molecules will act as plasticizers, allowing the onset of motion of the amide groups to occur at a lower temperature. The presence of clay within the polymer appears to have the opposite effect. The hydroxyl groups of the organic modifier cation on the clay platelet surface may form hydrogen bonds with the amide groups of the nylon 6. This will have the effect of restricting the onset of motion in the amide groups: the greater the concentration of clay, the greater the restriction effect. Therefore, the β-relaxation temperature will shift to a higher temperature with increasing clay concentration (Fig. 10).

The effect of the addition of nanoclay on the bending modulus can be observed in Figures 11 and 12, which show E' versus temperature and E' versus clay concentration at −95°C, respectively. An enhancement in E' can be observed with increasing clay concentration from 1 to 4 wt %. There is a dip in E' at 5 wt % that is likely due to the presence of intercalated rather than exfoliated clay platelets in the sample as verified by X-ray measurements.

Differential scanning calorimetry

Nonisothermal

Each nylon 6 and nylon 6/Cloisite 30B nanocomposite sample was heated, cooled, and heated again to obtain thermodynamic data. Heating scans were analyzed for glass transition temperature, T_g, melting temperature, T_m, and heat of fusion, ΔH_m, while cooling scans were used to obtain the crystallization temperature, T_c.

In Figure 13, the nonisothermal cooling scans for each nylon 6/clay nanocomposite sample are shown and the peak observed in each represents the crystallization of the sample as it was cooled from its first heating. The peak crystallization temperature for each sample is noted in Table II and it can be seen that the crystallization temperature is higher for the pure nylon 6 sample than that for the nanocomposite samples. This is an indication of the clay retarding the crystallization process of the polymer as it cools by limiting chain mobility. This phenomenon was further explored by an isothermal crystallization DSC experiment that is detailed in the following section.

Figure 14 and data from Table II show that peak melting temperature remains constant for all samples, at

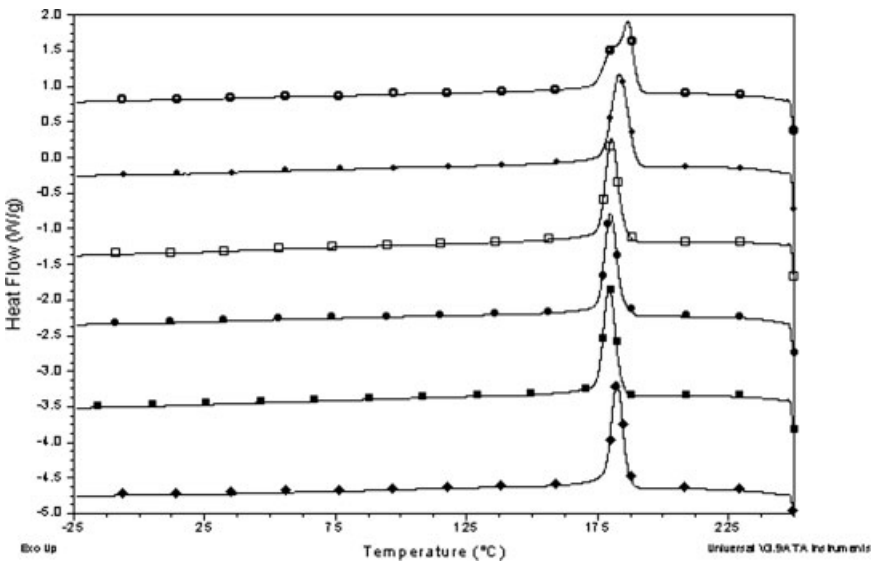

Figure 13 DSC scans for nonisothermal cooling of nylon 6/Cloisite 30B nanocomposite samples. (○) 0 wt %; (+) 1 wt %; (□) 2 wt %; (●) 3 wt %; (■) 4 wt %; (◆) 5 wt %

TABLE II
DSC Data for Nylon 6/Cloisite 30B Nanocomposite Samples

Clay concentration (wt %)	First heating		Cooling		Second heating	
	T_m (°C)	ΔH_m (J g^{-1})	T_c (°C)	ΔH_c (J g^{-1})	T_m (°C)	ΔH_m (J g^{-1})
0	215	73	*182*/187	69	*211*/218	59
1	215	69	183	72	*211*/217	61
2	220	87	180	63	*210*/217	48
3	221	76	180	61	*210*/218	47
4	220	85	179	63	*209*/218	54
5	212	71	182	66	*210*/218	55

Values in italic represent minor low temperature endo/exotherms.

approximately 218°C, regardless of clay concentration. This is consistent with work by Fornes et al.[31] on melt-mixed nylon 6/clay nanocomposites. The appearance of a shoulder on the melting peak at approximately 210°C may be an indication of the formation of the γ-form of nylon 6 as the sample is rapidly cooled during the cooling scan. The lower temperature of the γ-form is due to lower crystalline density and increased entropy of melting associated with the reduction in trans-conformational bonding compared to the α-form. The presence of the shoulder on the pure nylon 6 sample indicates that the formation of the γ-form in the nanocomposite is not caused by the presence of the clay but by the thermal conditions during crystallization.

Isothermal crystallization

The isothermal crystallization behavior of pure nylon and nylon 6/Cloisite 30B nanocomposite samples was examined at 195°C. Each sample was heated to 250°C to melt and the temperature rapidly decreased to 195°C. The samples were then allowed to crystallize for 60 min. The results are shown in Figure 15.

There is a definite retardation of the rate of crystallization in the nanocomposite samples when compared with that of the pure nylon 6 sample. Even at low clay concentrations, there is a marked increase in peak crystallization time from 4 min for the pure nylon 6 sample to approximately 6 min for the nanocomposite samples from 1 to 3 wt %. The exfoliated clay platelets hinder the movement of the polyamide chains as they attempt to align themselves into lamellae. The crystallization time for the 4 wt % sample increases further to nine minutes because of the increased amount of clay present. The *in situ* polymerization method that is used to synthesize these samples may have caused polyamide molecules to be tethered to the surface of the clay platelets. The hydroxyl groups present on the organic modifier cation may react with monomer during polymerization. The tethered chains will have greatly restricted mobility and this will further contribute to the decrease in crystallization rate of the nanocomposite samples. The 5 wt % sample also shows a decreased crystallization rate when compared with the pure nylon 6 sample but the crystallization time is lower than for the 4 wt % sample. This

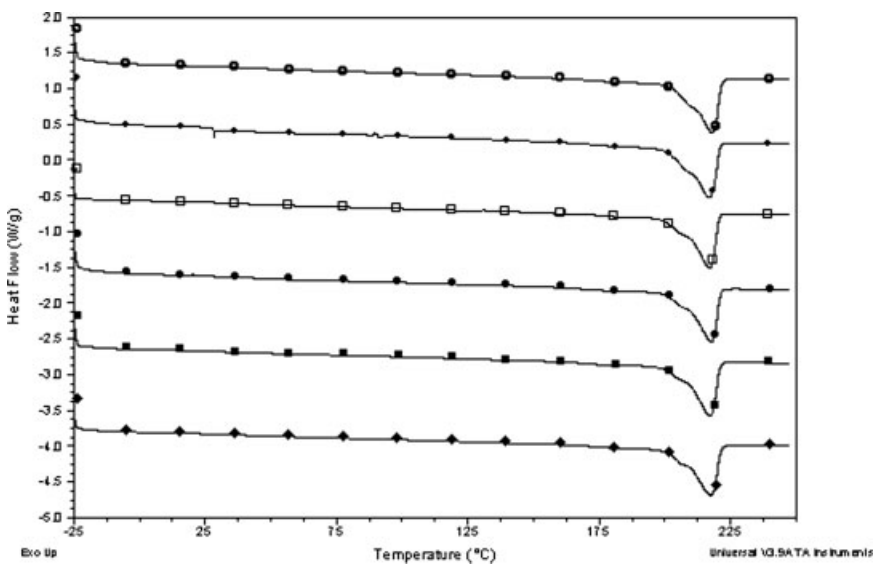

Figure 14 DSC scans for second heating of nylon 6/Cloisite 30B nanocomposite samples. (○) 0 wt %; (+) 1 wt %; (□) 2 wt %; (●) 3 wt %; (■) 4 wt %; (◆) 5 wt %.

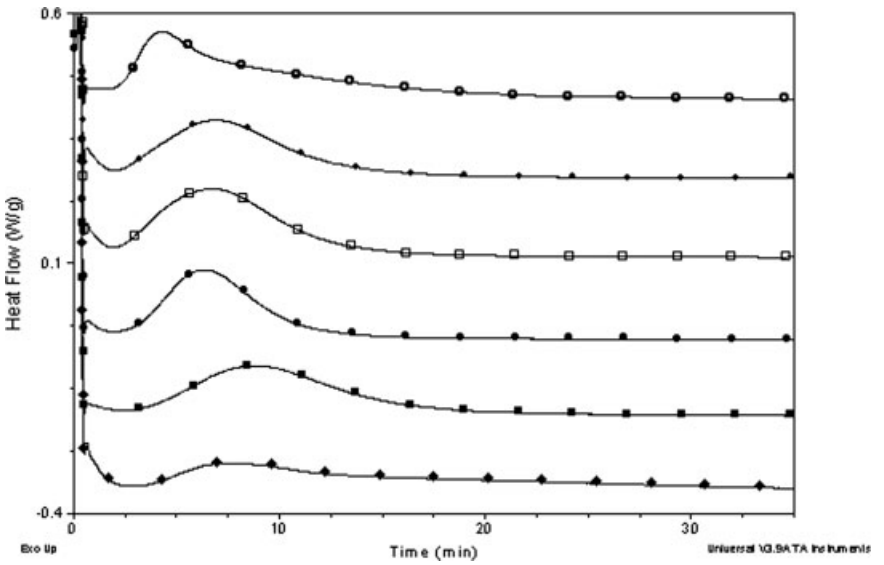

Figure 15 Crystallization isotherms for nylon 6/Cloisite 30 nanocomposite samples at 195°C. (●) 0 wt %; (+) 1 wt %; (□) 2 wt %; (●) 3 wt %; (■) 4 wt %; (◆) 5 wt %.

is perhaps an indication that the 5 wt % contains more lower molecular weight polymer than the rest of the nanocomposite samples.

Molecular weight

This last supposition was proven when each nanocomposite sample was measured by gel permeation chromatography. The results obtained are listed in Table III. The addition of the clay to nylon 6 has the effect of lowering the molecular weight of the polymer as the amount of clay present in the sample increases. The molecular weight distribution broadens and polydispersity increases as the clay concentration increases, which indicate that there are both high and low molecular weight molecules present. The increased presence of the low molecular weight material explains why the 5 wt % sample, when crystallized under nonisothermal and isothermal conditions, does not show the same retardation of the crystallization process that the samples with lower concentrations of clay demonstrate. The smaller polyamide 6 molecules are more mobile than the high molecular weight species, enabling them to crystallize at a faster rate.

The reason for the decrease in molecular weight as the clay concentration in the nanocomposite increases (Table III) is related to the organic modifier on the surface of the clay. Work on poly(caprolactone)/clay nanocomposite samples by Kiersnowski et al.[43] has shown the same increase in low molecular weight molecules with increasing clay loading. The decomposition of the organic modifier at temperatures of approximately 180°C[44], via a Hoffman elimination reaction, to produce amines is thought to be the reason for this reduction. The same reaction will occur in the nylon 6 nanocomposite samples as they are polymerized. The resulting amines can act as initiators, which react with the ε-caprolactam and can then polymerize further. This increase in the amount of initiator will have the effect of producing a greater number of low molecular weight polymer chains. Therefore, the reason for increase in low molecular weight material in the nylon 6 nanocomposite samples could be due for two reasons. First, the increase in the amount of initiator in the reacting system caused by the decomposition of the organic modifier to form amines, and second, the presence of the clay platelets themselves, which will hinder the diffusion of reacting species through the system.

CONCLUSIONS

Rheological measurements of sonicated Cloisite 30B in molten ε-caprolactam showed that exfoliation had occurred at concentrations from 1 to 5 wt %. Mixtures containing clay at concentrations of 2 wt % and higher showed a drop in the measured shear viscosity between initial shear runs and immediate

TABLE III
GPC Data for Nylon 6/Cloisite 30B Nanocomposite Samples

Clay concentration (wt %)	M_n (g mol^{-1})	M_w	Polydispersity (M_w/M_n)
0	69,700	132,000	1.9
1	58,200	129,000	2.2
2	54,000	150,000	2.8
3	45,100	157,000	3.5
4	35,400	137,000	3.9
5	23,200	157,000	6.8

repeat shear runs. This is attributed to a break down of an extensive amount of structure formed by the exfoliated platelets in the mixture during sonication. Repeat runs, after initial shearing, did not show the same level of viscosity and it is concluded that this structure cannot be reformed.

A method to synthesize nylon 6 and nylon 6/Cloisite 30B nanocomposites on a 10 g scale was developed. DMTA measurements showed the importance of a postcondensation step in the synthesis of samples as the glass transition temperature and bending modulus were shown to increase. Increasing the clay concentration present in a nanocomposite sample gave a slight increase in T_g and bending modulus. The β-relaxation temperature was shown to increase with increasing clay concentration. The organically modified clay platelets will interact and form hydrogen bonds with the amide groups of the nylon 6, restricting the onset of motion; an increase in the β-relaxation temperature is thus observed.

X-ray diffraction measurements of nylon 6/Cloisite 30B nanocomposite samples showed that the exfoliation of platelets had occurred during polymerization in samples of concentration 1–4 wt %. Results from the 5 wt % sample showed that some intercalated material was present. All samples were found to be in the α-crystalline form of nylon 6 rather than the γ-form, due to the long postcondensation step in the synthesis, which allows the chains to arrange themselves in the more thermodynamically stable form.

DSC scans showed that the nanocomposite samples formed the γ-crystalline form from the melt, with a fast cooling rate. Increasing clay concentration was shown to decrease the rate of crystallization of the nanocomposite by hindering chain mobility.

GPC measurements showed that the increasing concentration of clay in the sample has the effect of increasing the amount of low molecular weight polymer present. This is due to the increasing amount of organic modifier decomposing during the polymerization to form initiating amines and the clay hindering the movement of reacting species.

References

1. Fujiwara, S.; Sakamoto, T (assigned to Unitcha Ltd., Japan). Jpn. Pat. No. JP-A-51–109998 (1976).
2. Okada, A.; Fukushima, Y.; Kawasumi, M.; Inagaki, S.; Usuki, A.; Sugiyami, S.; Kurauchi, T.; Kamigaito, O (assigned to Toyota Motor Co., Japan). U.S. Pat. No. 4739007 (1988).
3. Usuki, A.; Kojima, Y.; Kawasumi, M.; Okada, A.; Fukushima, Y.; Kurauchi, T.; Kamigaito, O. J Mater Res 1993, 8, 1179.
4. Hay, J. N.; Shaw, S. J. Nanocomposites—Properties and Applications (from A Review of Nanocomposites 2000); http://www.azom.com/details.asp?ArticleID=921.
5. Solomon, M. J.; Almusallam, A. S.; Seefeldt, K. F.; Somwangthanaroj, A.; Varadan, P. Macromolecules 2001, 34, 1864.
6. Hoffmann, B.; Dietrich, C.; Thomann, R.; Friedrich, C.; Mulhaupt, R. Macromol Rapid Commun 2000, 21, 57.
7. Krishnamoorti, R.; Giannelis, E. P. Langmuir 2001, 17, 1448.
8. Wu, D. Z.; Wang, X. D.; Song, Y. Z.; Jin, R. G. J Appl Polym Sci 2004, 92, 2714.
9. Patel, S. S.; Larson, R. G.; Winey, K. I.; Watanabe, H. Macromolecules 1995, 28, 4313.
10. Becker, O.; Sopade, P.; Bourdonnay, R.; Halley, P. J.; Simon, G. P. Polym Eng Sci 2003, 43, 1683.
11. Kojima, Y.; Usuki, A.; Kawasumi, M.; Okada, A.; Kurauchi, T.; Kamigaito, O.; Kaji, K. J Polym Sci Part B: Polym Phys 1995, 33, 1039.
12. Medellin-Rodriguez, F. J.; Burger, C.; Hsiao, B. S.; Chu, B.; Vaia, R.; Phillips, S. Polymer 2001, 42, 9015.
13. Fornes, T. D.; Yoon, P. J.; Hunter, D. L.; Keskkula, H.; Paul, D. R. Polymer 2002, 43, 5915.
14. Fornes, T. D.; Hunter, D. L.; Paul, D. R. Macromolecules 2004, 37, 1793.
15. Fornes, T. D.; Yoon, P. J.; Keskkula, H.; Paul, D. R. Polymer 2001, 42, 9929.
16. Fornes, T. D.; Yoon, P. J.; Keskkula, H.; Paul, D. R. Polymer 2002, 43, 2121.
17. Cho, J. W.; Paul, D. R. Polymer 2001, 42, 1083.
18. Hasegawa, N.; Okamoto, H.; Kato, M.; Usuki, A.; Sato, N. Polymer 2003, 44, 2933.
19. Fornes, T. D.; Hunter, D. L.; Paul, D. R. Polymer 2004, 45, 2321.
20. Kojima, Y.; Usuki, A.; Kawasumi, M.; Okada, A.; Kurauchi, T.; Kamigaito, O. J Polym Sci Part A: Polym Chem 1993, 31, 1755.
21. Kojima, Y.; Usuki, A.; Kawasumi, M.; Okada, A.; Kurauchi, T.; Kamigaito, O. J Polym Sci Part A: Polym Chem 1993, 31, 983.
22. Yang, F.; Ou, Y. C.; Yu, Z. Z. J Appl Polym Sci 1998, 69, 355.
23. Usuki, A.; Kojima, Y.; Kawasumi, M.; Okada, A.; Fukushima, Y.; Kurauchi, T.; Kamigaito, O. J Mater Res 1993, 8, 1179.
24. Usuki, A.; Koiwai, A.; Kojima, Y.; Kawasumi, M.; Okada, A.; Kurauchi, T.; Kamigaito, O. J Appl Polym Sci 1995, 55, 119.
25. Rhoney, I.; Brown, S.; Hudson, N. E.; Pethrick, R. A. J Appl Polym Sci 2004, 92, 1335.
26. McIntyre, S.; Kaltzaharta, I.; Liggat, J. J.; Pethrick, R. A.; Rhoney, I. Industrial and Engineering Chemistry Research 2005, 44, 8573.
27. McAlpine, M.; Hudson, N. E.; Liggat, J. J.; Pethrick, R. A.; Pugh, D.; Rhoney, I. J Appl Polym Sci 2006, 99, 2614.
28. Ryu, J. G.; Park, S. W.; Kim, H.; Lee, J. W. Mater Sci Eng C: Biomimetic Supramol Syst 2004, 24, 285.
29. Delozier, D. M.; Orwoll, R. A.; Cahoon, J. F.; Johnston, N. J.; Smith, J. G.; Connell, J. W. Polymer 2002, 43, 813.
30. Yoonessi, M.; Toghiani, H.; Kingery, W. L.; Pittman, C. U. Macromolecules 2004, 37, 2511.
31. Fornes, T. D.; Paul, D. R. Polymer 2003, 44, 3945.
32. Liu, L.; Qi, Z.; Zhu, X. J Appl Polym Sci 1999, 71, 1133.
33. Kojima, Y.; Usuki, A.; Kawasumi, M.; Okada, A.; Fukushima, Y.; Kurauchi, T.; Kamigaito, O. J Mater Res 1993, 8, 1185.
34. VanderHart, D. L.; Asano, A.; Gilman, J. W. Chem Mater 2001, 13, 3781.
35. VanderHart, D. L.; Asano, A.; Gilman, J. W. Chem Mater 2001, 13, 3796.
36. Lincoln, D. M.; Vaia, R. A.; Wang, Z. G.; Hsiao, B. S. Polymer 2001, 42, 1621.
37. Li, J.; Zhou, C.; Wang, G.; Zhao, D. J Appl Polym Sci 2003, 89, 3609.
38. Sisko, A. W. Ind Eng Chem 1958, 50, 1789.
39. Einstein, A. Annalen Physik 1906, 19, 289.
40. Einstein, A. Annalen Physik 1911, 34, 591.
41. Kyotani, M.; Mitsuhashi, S. J Polym Sci Part A: Polym Chem 1972, 10, 1497.
42. Pramoda, K. P.; Liu, T. X. J Polym Sci Part B: Polym Phys 2004, 42, 1823.
43. Kiersnowski, A.; Piglowski, J. Eur Polym J 2004, 40, 1199.
44. Xie, W.; Gao, Z. M.; Pan, W. P.; Hunter, D.; Singh, A.; Vaia, R. Chem Mater 2001, 13, 2979.